NSRRC-Jo 4688 (2015)

Soft Matter

PAPER

View Article Online
View Journal | View Issue

Published on 22 January 2015. Downloaded by National Center for High-Performance Computing on 13/04/2015 04:12:35.

CrossMark click for updates

Cite this: *Soft Matter*, 2015, 11, 2237

A time-resolved study on the interaction of oppositely charged bicelles – implications on the charged lipid exchange kinetics†

Po-Wei Yang,[a] Tsang-Lang Lin,*[a] Yuan Hu[a] and U-Ser Jeng[b]

Time-resolved small-angle X-ray scattering was applied to study charged lipid exchange between oppositely charged disc-shaped bicelles. The exchange of charged lipids gradually reduces the surface charge density and weakens the electrostatic attraction between the oppositely charged bicelles which form alternately stacked aggregates upon mixing. Initially, at a high surface charge density with almost no free water layer between the stacked bicelles, fast exchange kinetics dominate the exchange process. At a later stage with a lower surface charge density and a larger water gap between the stacked bicelles, slow exchange kinetics take over. The fast exchange kinetics are correlated with the close contact of the bicelles when there is almost no free water layer between the tightly bound bicelles with a charged lipid exchange time constant as short as 20–40 min. When the water gap becomes large enough to have a free water layer between the stacked bicelles, the fast lipid exchange kinetics are taken over by slow lipid exchange kinetics with time constants around 200–300 min, which are comparable to the typical time constant of lipid exchange between vesicles in aqueous solution. These two kinds of exchange mode fit well with the lipid exchange models of transient hemifusion for the fast mode and monomer exchange for the slow mode.

Received 28th December 2014
Accepted 21st January 2015

DOI: 10.1039/c4sm02886d

www.rsc.org/softmatter

Introduction

The cell functions in an organism highly depend on the physical and chemical properties of the biological membrane, such as the transportation of general nutrients and waste through the membrane, as well as the delivery of genetic material or drugs.[1–4] Membrane properties depend highly on the lipid composition. Lipid transportation and lipid exchange are important biological processes for maintaining the lipid composition. Defects in lipid trafficking and incorrect lipid distributions in membranes can result in severe diseases.[5,6] However, knowledge on lipid transport or exchange kinetics is still limited and it is essential to understand lipid exchange mechanisms.[7] The movement of lipids among different bilayers is very diversified. Intra-bilayer lipid transfer includes lateral diffusion and flip-flop between the two leaflets of the bilayer.[8] As for inter-bilayer lipid exchange, there are several pathways, including monomer diffusion through the aqueous phase,[9] inverse flip-flop *via* transient contact,[6] lateral diffusion when hemifusion occurs and direct insertion.[7,10] Several factors affect inter-bilayer lipid exchange kinetics, such as concentration, temperature,[11] ionic strength,[12] and lipid species as well as the presence of other molecules.[6,13,14] For example, lipids with shorter acyl chains, higher numbers of double bonds and charged head groups can significantly accelerate lipid movement.[15,16] Moreover, the ionic strength and temperature can also regulate the electrostatic interactions and also alter the activation energy for lipid movement.[11] It is widely accepted that the most efficient pathway of inter-bilayer lipid exchange is concentration dependent transient contact, which is significantly faster than diffusion through the aqueous phase due to its lower activation energy. The other key factor that controls lipid exchange is the contact modes of the two bilayers. A larger contact area was found to facilitate lipid exchange,[17,18] especially in the case of the exchange between the oppositely charged solid supported lipid bilayer (SLB) and unilamellar vesicles (ULVs). The short-range electrostatic attraction during transient contact leads to membrane flattening which increases the contact area and enhances the lipid exchange.[15,19]

For investigating the kinetics of lipid transfer, microscopy and spectroscopy techniques are often used to observe the interface-specific processes during membrane fusion.[7,19–22] Recently, there were several successful studies using time-resolved small-angle neutron scattering (TR-SANS) to look into lipid exchange kinetics by mixing deuterated lipid vesicles with protonated lipid vesicles.[11,23,24] Nagano and coworkers

[a]*Department of Engineering and System Science, National Tsing Hua University, Hsinchu, Taiwan, Republic of China. E-mail: tllin@mx.nthu.edu.tw; Fax: +886-3-5728445; Tel: +886-3-5742671*

[b]*National Synchrotron Radiation Research Center (NSRRC), Hsinchu, Taiwan, Republic of China*

† Electronic supplementary information (ESI) available. See DOI: 10.1039/c4sm02886d

Published on 22 January 2015. Downloaded by National Center for High-Performance Computing on 13/04/2015 04:12:35.

investigated the exchange of zwitterionic lipids among small lipid bilayer nanodiscs consisting of a deuterated DMPC bilayer core and an apolipoprotein A-I (apoA-I) rim.[23,24] The lipid transfer rate was found to be about 20 times faster than the vesicle system through an entropically favorable process. As for studies on charged lipid exchange, there have been studies using a quartz crystal microbalance with a dissipation monitor (QCM-D) to check the entire attachment–transfer–detachment (ATD) time interval, t_{int}, of charged ULVs adsorbed on an oppositely charged SLB.[15,17,18] Kasemo and coworkers found that the charged ULVs took several to tens of minutes for the whole ATD process.[17,18] The time-scale of the charged lipid exchange (neutralization) among oppositely charged bilayers is significantly shorter than the lipid exchange between zwitterionic ULVs in aqueous solution. For the charged lipid exchange, short range electrostatic interactions must play a key role and the contact modes should also be important.

The investigation on lipid exchange could be greatly simplified by using disc-like bilayers, such as nanodiscs or disc-like bicelles, since the effects of curvature and flip-flop on the lipid exchange could all be eliminated.[25,26] The inner and outer leaflets of ULVs are asymmetric but for the two leaflets of the disc-like bicelles they are basically identical, both facing the outer environment and without curvature. Bicelles are typically formed by mixing long-chain lipids with short-chain lipids in aqueous solution.[27–31] At suitable long-chain lipid to short-chain lipid ratios, bicelles can form spontaneously with high size uniformity and structural stability. The temperature needs to be kept below the long-chain lipid hydrocarbon chain melting temperature to prevent the bicelles from fusing into vesicles. The planar bilayer core of the bicelle is formed by the long-chain lipids while the short-chain lipids form a protecting ring around the rim of the disc bilayer core.[29] Bicelles have been widely and successfully used in nuclear magnetic resonance (NMR) studies of membrane associated molecules since they can mimic lipid membranes and can also be easily oriented in magnetic fields for NMR studies.[32,33] Other than use as model membrane systems, recently bicelles have also been used in biomedical applications, such as drug delivery and DNA encapsulation.[25,26,34] As discussed, bicelles are ideal for investigating lipid exchange kinetics. In this report, the charged lipid exchange among oppositely charged bicelles at close contact was investigated by time-resolved small-angle X-ray scattering (TR-SAXS). As mentioned, using disc-shaped bicelles could eliminate the effects of flip-flop and curvature on the lipid exchange kinetics. Upon mixing, the oppositely charged lipid bicelles formed alternately stacked aggregates immediately. The number of stacked layers was correlated to the bicelle surface charge density. The exchange of charged lipids gradually reduced the surface charge density and caused the stacked bicelle aggregates to become shorter and shorter. Eventually, the stacked bicelles all dismantled into free bicelles once they were all neutralized. Following the structural evolution of the stacked bicelle aggregates as a function of time revealed the trend of the charged lipid exchange process between oppositely charged bicelles in close contact.

Experimental section

Materials and sample preparation

All lipids used in this study were purchased from Avanti Polar Lipids, Inc. The disc-like bicelles were formed by mixing the zwitterionic long-chain lipid 1,2-dipalmitoyl-*sn-glycero*-3-phosphocholine (DPPC) and the short-chain lipid 1,2-diheptanoyl-*sn-glycero*-3-phosphocholine (diC7PC) in aqueous solution. At the long to short chain lipid molar ratio of 3, these lipids self-assembled into disc-shaped bicelles with a planar long-chain lipid bilayer core surrounded by a short-chain lipid rim.[27–31,35] The typical bicelle diameter was around 20 nm with a bilayer thickness of about 6 nm at room temperature.[35] The total long-chain lipid concentration was kept at 10 mM (including the charged lipids) and the diC7PC concentration was kept at 3.3 mM in this study. The surface charge density of the bicelle was controlled by doping/replacing some of the zwitterionic DPPC with anionic 1,2-dipalmitoyl-*sn-glycero*-3-phospho-(1′-*rac*-glycerol) (DPPG) or cationic cholesterol 3β-[*N*-(*N*′,*N*′-dimethylaminoethane)-carbamoyl] (DC-cholesterol) in order to form negatively or positively charged bicelles, respectively. Three charge doping percentages, 7.5%, 15% and 30%, were used in this study in order to compare the effects of the membrane surface charge density on the bilayer interactions and lipid exchange kinetics.

Small-angle scattering (SAS) and transmission electron microscopy (TEM)

The TR-SAXS measurements were conducted at the BL23A of the National Synchrotron Radiation Research Center (NSRRC),[36] Hsinchu, Taiwan, to record the structural evolution of the mixed aggregates formed by the oppositely charged bicelles. The X-ray photon energy and sample to detector distance were 14 keV and 2.8 m, respectively, in order to cover a Q range of 0.008–0.35 Å^{-1}. Here, the scattering vector Q is equal to $(4\pi/\lambda)\sin(\theta/2)$, where λ is the X-ray wavelength and θ is the scattering angle. The liquid samples were sealed in a sample cell with Kapton-walled windows. The samples were kept at 25 °C during the measurements. Scattered X-rays were collected by a MarCCD detector. The collected 2D data were circular averaged to obtain the 1D scattering intensity *versus* scattering vector distribution. The measured scattering intensities were corrected for the detector sensitivity and background, and normalized to obtain the absolute scattering cross sections. For preparing the TEM samples, the samples were first diluted, then dripped onto a copper grid with a supported membrane. Any extra solution was sopped out by filter paper. In order to enhance the sample contrast, negative-staining was applied to the samples by adding uranyl acetate (1 wt%) for 30 seconds. TEM images were taken at an e-beam energy of 100 kV by the JEOL JEM-1230 of Chang Gung University, Taiwan.

Results and discussion

Fig. 1 shows the TEM images of the 15% charged cationic and anionic bicelles, and the mixture of the mixed cationic and

 This journal is © The Royal Society of Chemistry 2015

Published on 22 January 2015. Downloaded by National Center for High-Performance Computing on 13/04/2015 04:12:35.

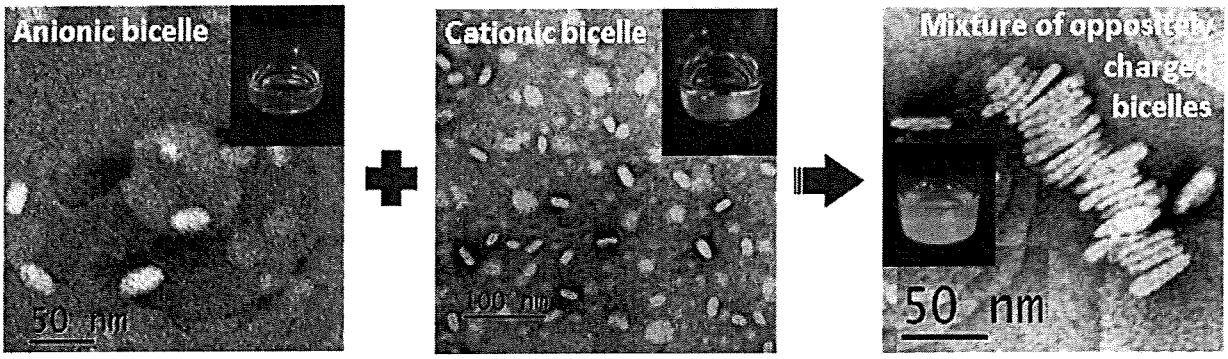

Fig. 1 The TEM images of the bicelles and the photos of the sample solutions. For preparing the TEM samples, the samples were first diluted, then dripped onto a copper grid with a supported membrane. The anionic bicelle sample contains 1.5 mM DPPG, 8.5 mM DPPC and 3.3 mM diC7PC (15% charged anionic bicelle), whereas the cationic sample contains 1.5 mM DC-cholesterol, 8.5 mM DPPC and 3.3 mM diC7PC (15% charged cationic bicelle). The anionic bicelles and the cationic bicelles have a uniform size of around 20 nm in diameter. Both the anionic and cationic bicelles are respectively well dispersed in the solutions and the sample solutions look clear. Right after mixing the anionic bicelles with the cationic bicelles, one-dimensionally stacked aggregates of the oppositely charged bicelles form immediately. Right after mixing, the mixed sample solution looks opaque.

anionic bicelles a few minutes after mixing. When the prepared bicelles with equal but oppositely charged doping were mixed at equal volume, one-dimensionally stacked bicelle aggregates formed immediately and the solution became slightly opaque. The exchange of charged lipids decreased the net bicelle surface charge density gradually and weakened the charge attraction between the oppositely charged bicelles. As a result, the bicelle stacks became shorter and the bicelles in the stack were also less tightly bound resulting in a larger d-spacing. Eventually, all the bicelles became free isolated bicelles with a net charge of around zero.

In order to quantitatively describe the evolution of the size of the bicelle stacks, a model of bicelle stacks plus free bicelles was used to simulate the scattering profiles obtained by TR-SAXS. The scattering profile can be described by $I(Q) = n_{p,1}P(Q)S(Q) + n_{p,2}P(Q)$, where $P(Q)$ is the core–shell disc form factor for a bicelle,[35,37] $S(Q)$ is the structure factor for one-dimensionally stacked discs proposed by Kratky and Porod in 1949,[38] $n_{p,1}$ is the number density of the bicelles forming the stacked aggregates, and $n_{p,2}$ is the number density of the free bicelles. The ratio of the free bicelles to those in the stacked aggregates is defined as C_1. The fitting results are shown in Fig. S1 and Table T1–T3 in the ESI.†

Fig. 2 shows the representative TR-SAXS profiles for the 15% charge doping system at several time intervals, together with the schematics. At the beginning when the oppositely charged bicelles were mixed in the solution, long stacks of alternating positively and negatively charged bicelles formed immediately through short-range electrostatic attraction forces. Once the oppositely charged bicelles come into close contact, a relatively fast exchange of charged lipids can occur immediately. All the lipids, including zwitterionic and charged lipids can exchange and flip-flop spontaneously. However, in the present system, by using disc-like bicelles, the flip-flop of all lipid species and the exchange of zwitterionic lipids do not affect the surface charge density of the bicelles or the stacking of the oppositely charged bicelles. As a result, the size of the stacked structure of the oppositely charged bicelles is correlated only to the exchange of the charged lipids. When the charged lipids switch to the oppositely charged bicelles, the cationic and anionic lipids form association pairs due to the strong electrostatic interactions

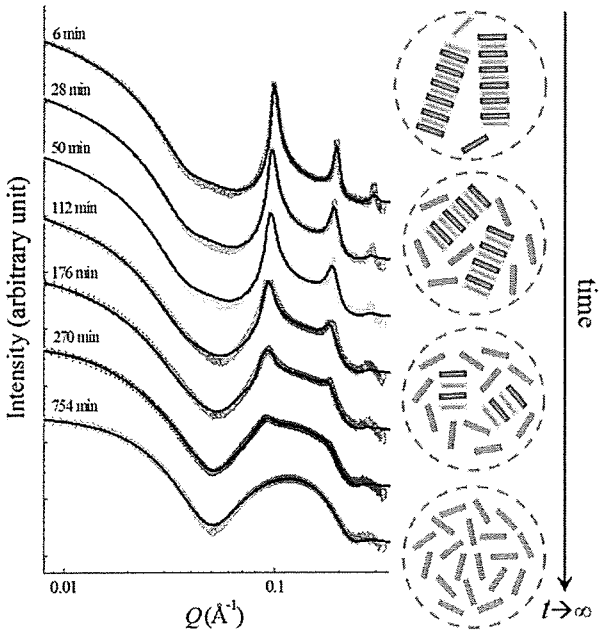

Fig. 2 The representative TR-SAXS profiles of mixing oppositely charged bicelles of 15% charge doping at room temperature and the schematics of the evolution of the mixed bicelle system at different stages after mixing. The anionic bicelle contains 1.5 mM DPPG, 8.5 mM DPPC and 3.3 mM diC7PC, whereas the cationic sample contains 1.5 mM DC-cholesterol, 8.5 mM DPPC and 3.3 mM diC7PC. Right after mixing, the oppositely charged lipid bicelles form alternately stacked aggregates. Due to the charged lipid exchange, the stacked aggregates gradually dissociate into free bicelles.

Published on 22 January 2015. Downloaded by National Center for High-Performance Computing on 13/04/2015 04:12:35.

between the two oppositely charged lipids and the entropy increases due to the release of their respective counter-ions. The strong electrostatic interactions drive the charged lipids to switch side to lower the free energy and maximize the entropy. The first several time frames of all cases exhibit a set of Bragg's diffraction peaks at around $Q = 0.1$ Å^{-1}, 0.2 Å^{-1} and 0.3 Å^{-1} originating from the constructive interference of the periodic structure of the stacked bicelle aggregates. The diffraction peak intensities decrease gradually as time increases, which indicates that the mean stack number of the bicelles decreases with time. The peak position also shifts gradually to lower Q with time which indicates that the d-spacing between neighboring bicelles increases with time. The sharp diffractions gradually disappear and eventually the scattering profiles turn into only the free bicelle form factor. The dissociation of the stacked bicelles with time is due to the neutralization process caused by the exchange of the charged lipids.

The obtained d-spacing, mean stack number N and $C_1/(1 + C_1)$ are plotted as a function of time as shown in Fig. 3. At the beginning, the d-spacing is around 6.28, 6.44, and 6.68 nm, respectively for the cases of charge doping of 30%, 15%, and 7.5%. The d-spacing of the bicelle stacks was found to be smaller for the cases with higher bicelle surface charge densities. The d-spacing consists of one lipid bilayer thickness, two thin layers of hydration water and a layer of free water. As shown in Fig. 3, the increase of the d-spacing is faster in the beginning and the increase gradually slows down at the later stage.

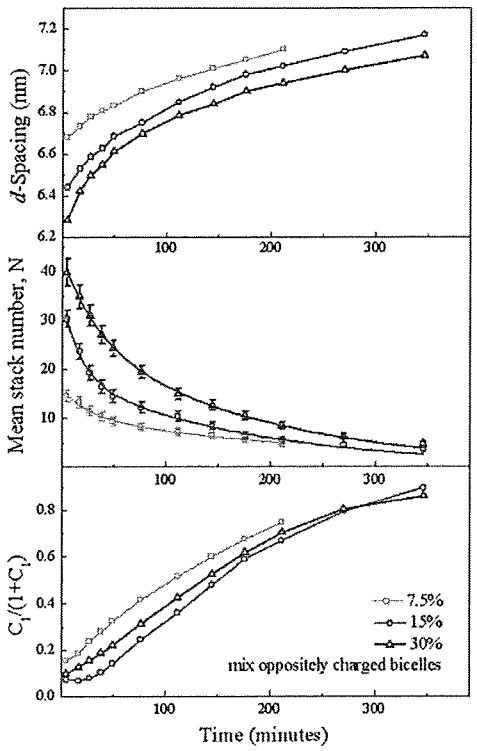

Fig. 3 Plots of the deduced d-spacing, mean bicelle stack number, and the fraction of free bicelles to all bicelles as a function of time.

The ratio of free bicelles to total bicelles, $C_1/(1 + C_1)$, which is also an indicative index for tracing the transformation of bicelle stacks to free bicelles, increases as a function of time. The fraction of free bicelles increases toward 100% in a time scale of a few hours. The increase of free bicelles also implies the gradual neutralization and the dissociation of the bicelle stacks. The time-dependent evolution of the number of bicelles in one stacked bicelle aggregate (the mean aggregation number) $N(t)$ is also indicative of the charge neutralization induced by the charged lipid exchange. As shown in Fig. 3, the time-dependent evolution of the mean aggregation number $N(t)$ as obtained from analyzing the TR-SAXS profiles drops sharply in the beginning and the rate of decrease slows as time goes on. $N(t)$ can be well represented by a double-exponential decay function:

$$N(t) = A_1 \, e^{-t/t_1} + A_2 \, e^{-t/t_2}. \quad (1)$$

This means that there are two distinct kinetics modes of the charged lipid exchange. One is a fast mode and the other one is a slow mode. The fitting results are listed in Table 1.

As shown in Table 1, the fast mode has time constants of around 20–40 min, and the slow mode has much longer time constants of around 200–300 min. For each mode, the doping percentage of charged lipids has some effects on the time constants due to the differences in the strength of the electrostatic interactions as well as the physical properties of the bilayers, such as the bending modulus and molecular structure due to the differences in the composition of the bicelles. For example, the doping of DC-cholesterol would lower the membrane fluidity and further lift the activation energy of the lipid exchange.[39] For the fast mode, the time constant decreases from 31 min to 20 min as the charge doping percentage is increased from 7.5% to 15%. The decrease in the time constant seems to be due to the stronger electrostatic interactions for the increased surface charge density. However, despite the increased electrostatic interactions, the time constant is increased from 20 min to 43 min when the doping percentage is further increased from 15% to 30%. It is likely that the higher doping percentage of 30% would significantly alter the membrane properties and the lipid exchange would also be affected. As for the slow mode, the time constant is around 298 min for the 7.5% charge doping case, and 201 min and 213 min for the 15% and 30% charge doping cases, respectively. For the slow mode, the time constant is obviously smaller for the higher charge doping cases.

As determined from fitting the TR-SAXS data, at the beginning, the average water gap between the stacked bicelles was

Table 1 Parameters of fitting $N(t)$ with a double-exponential decay function

	7.5%	15%	30%
A_1	6.0 ± 1.2	18.9 ± 1.1	20.5 ± 1.8
t_1 (min)	31.2 ± 9.6	20.3 ± 2.6	43.4 ± 4.1
A_2	9.9 ± 1.3	16.9 ± 1.1	22.8 ± 1.9
t_2 (min)	298 ± 70	201 ± 17	213 ± 16

This journal is © The Royal Society of Chemistry 2015

Published on 22 January 2015. Downloaded by National Center for High-Performance Computing on 13/04/2015 04:12:35.

found to be around 0.91, 0.67 and 0.51 nm, respectively for the charge doping percentages of 7.5%, 15%, and 30%. Such small average water gaps correspond to just 2–3 water molecule layers,[40] which is nearly only the hydration water layers. The oppositely charged bicelles are tightly bound together at the beginning when the surface charge density is high. As indicated by the increase of the *d*-spacing with time, the average water gap gradually increases with time due to the lowering of the surface charge density as the charged lipid exchange proceeds. It seems that the fast mode of the charged lipid exchange is correlated with the small water gap. The close contact between the oppositely charged bicelles facilitates the charged lipid exchange driven by strong electrostatic interactions. When there is almost no free water layer between the bicelles, the lipid bilayer interactions are greatly enhanced. Efficient charged lipid exchange is only found when the oppositely charged bicelles are in close contact *via* short-range electrostatic attractions. The obtained time constant of the fast mode is around tens of minutes which is comparable with the interaction time interval of charged ULV bound on oppositely charged SLB measured by QCM-D.[17,18] As suggested by Wikström *et al.*, transient formation of hemifusion could occur upon close contact of the vesicle bilayers under strong electrostatic interactions.[17]

The fast mode is taken over by the slow mode after about one hour. In this latter stage of evolution, the *d*-spacing as well as the average water gap becomes larger. The larger *d*-spacing means that a free water layer starts to exist between the bound bicelles. The exchange of the charged lipids at this stage would be more difficult since the lipids, one by one *via* monomer exchange, would need to get into the free water layer first before they can get into the opposite side as suggested by Wikström *et al.*[17] The time constant for the slow mode is thus comparable to the typical lipid exchange time constant between ULVs in aqueous solution.[11] The lipid exchange time constant of the zwitterionic DMPC/d-DMPC vesicles at 37 °C as determined by the TR-SANS study is 217 min which is close to the 200–300 min time constant for the slow mode of this study. When the bicelles are loosely bound as in the slow mode stage, the charged lipid exchange exhibits slow exchange kinetics as that of the zwitterionic lipids in the vesicle system. This could be due to the fact that the lipids need to diffuse through the free water layer between the loosely bound bicelles in the later stage of the neutralization process which is somewhat similar to the lipid exchange between the vesicles in aqueous solution. For the lower charge doping case of 7.5%, the component of the fast mode is significantly smaller than its slow mode, as listed in Table 1. The charged lipid exchange process for the 7.5% charge doping case, as viewed by the change of the *d*-spacing and mean aggregation number with time, would be close to the later evolution stages of the 15% and 30% charge doping cases. The time evolution of the mean aggregation number $N(t)$ of the 7.5% case can be shifted in time, about 50 min and 75 min, respectively, to approximately match the time evolution of $N(t)$ at the later stages of the 15% and 30% cases.

Conclusions

In summary, using charged disc-shaped bicelles enabled us to trace the exchange of only charged lipids and to avoid the flip-flop and curvature effects on lipid exchange. The exchange of charged lipids was found to possess two kinds of exchange kinetics, a fast mode dominates in the beginning and a slow mode takes over in the later stage. Initially, at a high surface charge density with almost no free water layer between the bound bicelles, fast exchange kinetics dominate the exchange process. At the later stage with a lower surface charge density and wider water gaps between the bicelles, slow exchange kinetics take over. This is the first time such two-stage exchange kinetics have been observed in a lipid bilayer system. These two kinds of exchange mode fit well with the lipid exchange models of transient hemifusion for the fast mode and monomer exchange for the slow mode.[17] It is concluded that the water gap with or without the free water layer as well as electrostatic interactions are critical factors for determining the charged lipid exchange kinetics between lipid membranes in close contact. The present observation could be useful for understanding membrane fusion mechanisms and also lipid exchange during vesicle collisions. This study could also be extended to study the role of proteins in inducing membrane fusion, where proteins are thought to reduce the distance between the two bilayers during vesicle contact.[41] The bicelle interactions investigated here should also be useful in applying bicelles for studying various membrane interactions with antimicrobial peptides[42,43] and amyloid peptides.[44–46]

Acknowledgements

We would like to thank the NSRRC for providing the SAXS beam time and the help during the measurements. This research is supported by the project NSC 102-2113-M-007-013 and MOST 103-2113-M-007-014-MY2 (T.-L. Lin). This research is also partly supported by the Frontier Research Center on Fundamental and Applied Sciences of Matters of National Tsing Hua University.

References

1 J. O. Rädler, I. Koltover, T. Salditt and C. R. Safinya, *Science*, 1997, 275, 810.
2 J. J. Lu, R. Langer and J. Chen, *Mol. Pharm.*, 2009, **6**, 763.
3 I. A. Khalil, K. Kogure, H. Akita and H. Harashima, *Pharmacol. Rev.*, 2006, **58**, 32.
4 L. V. Chernomordik and M. M. Kozlov, *Nat. Struct. Mol. Biol.*, 2008, **15**, 675.
5 S. Lev, *Cold Spring Harbor Perspect. Biol.*, 2012, **4**, a013300.
6 W. A. Prinz, *Cell*, 2010, **143**, 870.
7 D. P. Pantazatos and R. C. MacDonald, *J. Membr. Biol.*, 1999, **170**, 27.
8 R. Machan and M. Hof, *Biochim. Biophys. Acta, Biomembr.*, 2010, **1798**, 1377.
9 R. F. Brown, *Biochim. Biophys. Acta, Rev. Biomembr.*, 1992, **1113**, 375.

Published on 22 January 2015. Downloaded by National Center for High-Performance Computing on 13/04/2015 04:12:35.

10 V. P. Zhdanov and B. Kasemo, *J. Phys. Chem. B*, 2007, **111**, 9428.
11 M. Nakano, M. Fukuda, T. Kudo, H. Endo and T. Handa, *Phys. Rev. Lett.*, 2007, **98**, 238101.
12 E. Yang and W. H. Huestis, *Biochemistry*, 1993, **32**, 12218.
13 R. Koynova and R. C. MacDonald, *Biochim. Biophys. Acta, Biomembr.*, 2005, **1714**, 63.
14 L. Estronca, M. J. Moreno, J. A. N. Laranjinha, L. M. Almeida and W. L. C. Vaz, *Biophys. J.*, 2005, **88**, 557.
15 T. Zhu, Z. Jiang and Y. Ma, *Colloids Surf., B*, 2012, **97**, 155.
16 J. T. Crowley, A. M. Toledo, T. J. LaRocca, J. L. Coleman, E. London and J. L. Benach, *PLoS Pathog.*, 2013, **9**, e1003109.
17 A. Wikström, S. Svedhem, M. Sivignon and B. Kasemo, *J. Phys. Chem. B*, 2008, **112**, 14069.
18 A. Kunze, S. Svedhem and B. Kasemo, *Langmuir*, 2009, **25**, 5146.
19 G. H. Lei and R. C. MacDonald, *Biophys. J.*, 2003, **85**, 1585.
20 V. MarchiArtzner, L. Jullien, L. Belloni, D. Raison, L. Lacombe and J. M. Lehn, *J. Phys. Chem.*, 1996, **100**, 13844.
21 R. D. Kornberg and H. M. McConnel, *Biochemistry*, 1971, **10**, 1111.
22 T. C. Anglin, M. P. Cooper, H. Li, K. Chandler and J. C. Conboy, *J. Phys. Chem. B*, 2010, **114**, 1903.
23 M. Nakano, M. Fukuda, T. Kudo, M. Miyazaki, Y. Wada, N. Matsuzaki, H. Endo and T. Handa, *J. Am. Chem. Soc.*, 2009, **131**, 8308.
24 S. Garg, L. Porcar, A. C. Woodka, P. D. Butler and U. Perez-Salas, *Biophys. J.*, 2011, **101**, 370.
25 P.-W. Yang, T.-L. Lin, Y. Hu and U. S. Jeng, *Soft Matter*, 2014, **10**, 2313.
26 P.-W. Yang, T.-L. Lin, T.-Y. Lin, C.-H. Yang, Y. Hu and U. S. Jeng, *Soft Matter*, 2013, **9**, 11542.
27 N. E. Gabriel and M. F. Roberts, *Biochemistry*, 1986, **25**, 2812.
28 T.-L. Lin, S. H. Chen, N. E. Gabriel and M. F. Roberts, *J. Am. Chem. Soc.*, 1986, **108**, 3499.
29 T.-L. Lin, C.-C. Liu, M. F. Roberts and S. H. Chen, *J. Phys. Chem.*, 1991, **95**, 6020.
30 J. Katsaras, T. A. Harroun, J. Pencer and M. P. Nieh, *Naturwissenschaften*, 2005, **92**, 355.
31 J. Bian and M. F. Roberts, *Biochemistry*, 1990, **29**, 7928.
32 U. H. N. Dürr, M. Gildenberg and A. Ramamoorthy, *Chem. Rev.*, 2012, **112**, 6054.
33 U. H. N. Dürr, R. Soong and A. Ramamoorthy, *Prog. Nucl. Magn. Reson. Spectrosc.*, 2013, **69**, 1.
34 L. Rubio, C. Alonso, G. Rodríguez, M. Cócera, C. López-Iglesias, L. Coderch, A. De la Maza, J. L. Parra and O. López, *Int. J. Pharm.*, 2013, **444**, 60.
35 P.-W. Yang, T.-L. Lin, Y. Hu and U. S. Jeng, *Chin. J. Phys.*, 2012, **50**, 349.
36 U.-S. Jeng, C. H. Su, C. J. Su, K.-F. Liao, W.-T. Chuang, Y.-H. Lai, J. W. Chang, Y. J. Chen, Y. S. Huang, M.-T. Lee, K. L. Yu, J. M. Lin, D. G. Liu, C. F. Chang, C. Y. Liu, C. H. Chang and K. S. Liang, *J. Appl. Crystallogr.*, 2010, **43**, 110.
37 S. R. Kline, *J. Appl. Crystallogr.*, 2006, **39**, 895.
38 O. Kratky and G. Porod, *J. Colloid Sci.*, 1949, **4**, 35.
39 H. Ohvo-Rekilä, B. Ramstedt, P. Leppimäki and J. P. Slotte, *Prog. Lipid Res.*, 2002, **41**, 66.
40 M. Ge and J. H. Freed, *Biophys. J.*, 2003, **85**, 4023.
41 M. Kogan, B. Feng, B. Norden, S. Rocha and T. Beke-Somfai, *Langmuir*, 2014, **30**, 4875.
42 A. Ramamoorthy, *Solid State Nucl. Magn. Reson.*, 2009, **35**, 201.
43 L. M. Gottler and A. Ramamoorthy, *Biochim. Biophys. Acta, Biomembr.*, 2009, **1788**, 1680.
44 N. Popovych, J. R. Brender, R. Soong, S. Vivekanandan, K. Hartman, V. Basrur, P. M. Macdonald and A. Ramamoorthy, *J. Phys. Chem. B*, 2012, **116**, 3650.
45 J. R. Brender, D. L. Heyl, S. Samisetti, S. A. Kotler, J. M. Osborne, R. R. Pesarub and A. Ramamoorthy, *Phys. Chem. Chem. Phys.*, 2013, **15**, 8908.
46 S. A. Kotler, P. Walsh, J. R. Brender and A. Ramamoorthy, *Chem. Soc. Rev.*, 2014, **43**, 6692.

This journal is © The Royal Society of Chemistry 2015